Accepted Manuscript

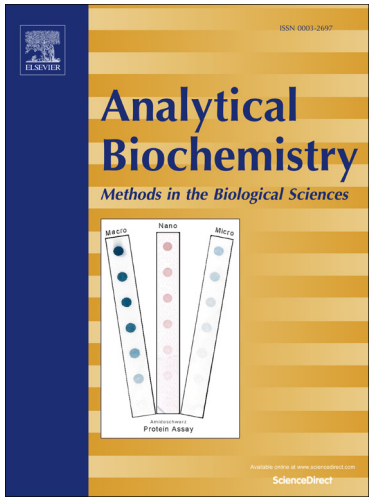

Eco-synthesis of graphene and its use to NADH sensing

Mahmoud Amouzadeh Tabrizi, Somayeh Jalilzadeh Azar

PII: S0003-2697(14)00197-3
DOI: http://dx.doi.org/10.1016/j.ab.2014.05.002
Reference: YABIO 11735

To appear in: *Analytical Biochemistry*

Received Date: 6 April 2014
Revised Date: 4 May 2014
Accepted Date: 6 May 2014

Please cite this article as: M.A. Tabrizi, S.J. Azar, Eco-synthesis of graphene and its use to NADH sensing, *Analytical Biochemistry* (2014), doi: http://dx.doi.org/10.1016/j.ab.2014.05.002

Category: Special tapics

Eco-synthesis of graphene and its use to NADH sensing

Mahmoud Amouzadeh Tabrizi[*a] and Somayeh Jalilzadeh Azar[b]

[a] Department of Chemistry, Razi University, Kermanshah, Iran

[b] Department of Microbiology, Islamic Azad University (Varamin-Pishva Branch), Varamin, Iran.

* *Corresponding author, Tel/fax:* (+98) 21-44042955, Email: mahmoud.tabrizi@gmail.com

Abstract

Here, we report a green and eco-friendly approach to synthesize reduced graphene oxide (rGO) via a mild hydrothermal process using malt as a reduced agent. The proposed method is based on the reduction of graphene oxide (GO) in malt solution by making use of the reducing capability of phenolic compounds that contained in malt solution. The obtained rGO was characterized by atomic force microscopy, UV-visible absorption spectroscopy, X-ray diffraction spectroscopy (XRD), Raman spectroscopy, Fourier transform infrared (FT-IR) spectroscopy, Atomic force microscopy (AFM), Scanning electron microscopy (SEM) and Transmission electron microscopy (TEM). Electrochemical impedance spectroscopy analysis revealed that the charge transfer resistance of rGO modified glassy carbon (GC) electrode was much lower than of the GC electrode. The electrochemical behavior of dihydronicotinamide adenine dinucleotide (NADH) on rGO modified GC electrode was investigated by cyclic voltammetry and amperommetry. Electrochemical experiments indicated that rGO/GC electrode exhibited an excellent electrocatalytic activity towards the NADH, which can be attributed to excellent electrical conductivity and high specific surface area of the rGO composite. The resulting biosensor showed highly sensitive amperometric response to NADH with a low detection limit (0.33μM).

Keywords: Green chemistry; Malt; Reduced graphene oxide; NADH

1. Introduction

The discovery of graphene by Andre Geim and Konstantin Novoselov in 2004 has generated a great and sustained interest in graphene and its applications [1]. Graphene, a single aromatic sheet of sp^2 bonded carbon, have been shown to possess unique electronic, optical, thermal, mechanical and catalytic properties, which are attractive for widely varied potential applications in many fields of science ranging from nano-electronics to biomedical devices.

In fact, most of the graphenes that were chemically synthesized contain other elements, such as oxygen, so it is more reasonable to call the graphene ‘‘reduced graphene oxide‘‘(rGO). This composite can be synthesized by various methods [2-6]. Among the current methods of the generating reduced graphene oxide, hydrazine and sodium borohydride are used for the chemical reduction of exfoliated graphene oxide (GO) [7, 8]. However, these reducing agents are unstable and dangerously toxic. Several groups investigated the synthesis of rGO with the eco-friendly methods, opening the door to application in nano-science [2-4, 9, 10].

Thus, the chemical reduction of exfoliated GO with green reducing agents have become a favorable topic for researchers. For example, reducing sugar [11], protein bovine serum albumin [12], heparin [13], poly(diallyldimethylammonium chloride) [14] and Plant extracts [15-17] performs well in reduction of GO. Therefore, an effective, low-cost and green reducing agent for chemical synthesis of soluble graphene is desirable. Surprisingly, these green reducing agents act as both reducing and stabilizing agent, thus the improvement in stability of rGO good solubility observed.

Malt is the third-most popular drink overall, after water and tea. The variability of the components and their occurrence in barely malts are dependent on the brand company. It has

been reported that the identified major components of barley malt from tuborg brand are maltose, dextrins, acetate, lactate, alanine, etanol and phenolic compounds [18].

Several reports are on antioxidant and antimicrobial properties of malt which is due to their ability to reduce free radical formation and scavenge free radicals [19-21]. It has been reported that the sources of natural antioxidants in malt are phenolic compounds.

The malt phenolic compounds are biocompatible, and mainly consisted of syringic acid, coumaric acid, ferulic acid, protocatechuic acid, vanillic acid, caffeic acid, p-hydroxybenzoic acid, tannic acid, epicatechin, and quercetin [22]. These compounds are excellent antioxidant agents because they can readily react with reactive oxygen species such as free radicals.

Upon oxidation, the phenol groups convert to their corresponding quinone forms that they are also biocompatible [23]. Previously, the phenolic compounds have been also used for green synthesis of nanoparticles [24-27]. According to previous reports, graphene exhibits excellent electron transfer promoting ability for some enzymes and excellent catalytic behavior toward biomolecule such as, dihydronicotinamide adenine dinucleotide (NADH) [28-33].

The determination of NADH is one of the important topics in biology, biochemistry and medicine. Several methods are available for the determination of NADH [34-37]. However, these methods are generally time-consuming, have a lack of sensitivity and a susceptibility to interference with other substances in analyte samples and are difficult for an automated detection. To overcome all these shortcomings, the electrochemical sensors based on carbon nanomaterials such as graphene and its derivatives are especially promising because of their simplicity, high sensitivity, selectivity and low over potential oxidation [28, 38-42].

In this paper, we demonstrate a simple method to prepare rGO sheets in aqueous media by malt as well as toxic agents. We made use of reducing capability of aromatic phenolic components of

malt for reduction of graphene oxide. The electrochemical behavior of NADH on rGO modified glassy carbon was also studied. The prepared biosensor exhibited lower detection limit and high sensitivity for NADH.

2. Experimental

2.1. Materials

All chemicals were of analytical reagent grade and used without further purification. High purity graphite powder (particle size < 0.1 mm), H_3PO_4, H_2SO_4, $KMnO_4$, HCl, KOH, KCl, $K_3[Fe(CN)_6]$, $K_4[Fe(CN)_6]$. Ethanol (96%) and ammonium hydroxide (25%) were obtained from Fluka (Buchs, Switzerland). NADH was obtained from Sigma. Non-alcoholic barley malt of Tuborg brand (Germany) was obtained from local malt. Double distilled water was used throughout.

2.2. Apparatus

UV-Visible absorption spectra were recorded using a single beam Pharmacia UV-vis spectrophotometer (Ultrospec, model 4000). Fourier Transform Infra-Red (FTIR) analysis was carried out using a Bruker (Germany) vector 22 spectrometer. Raman scattering was performed on a Almega Thermo Nicolet Dispersive Raman spectrometer using the second harmonic (532 nm) of a Nd:YLF laser source. Transmission electron microscopy (TEM) measurements were made on a HITACHI H-8100 EM with an accelerating voltage of 200 kV. Scanning electron microscopy (SEM) was performed with a Philips instrument, Model XL-30 (Eindhoven, The Netherlands). The surface morphology of the products was characterized using a DME DualScope Scanner DS 95-200 (Herlev, Denmark) atomic force microscopy (AFM). X-ray

diffraction (XRD) spectra were obtained using a D8ADVANCE (Bruker, Germany) using Cu Kα (1.5406 Å) radiation. Cyclic voltammetry was performed using an Autolab potentiostat-galvanostat model PGSTAT30 (Utrecht, The Netherlands) with a conventional three electrode set-up, in which a bare GC electrode or rGO modified GC electrode, an Ag|AgCl|KCl_{sat} and a platinum rod served as the working, reference and auxiliary electrodes, respectively. Electrochemical impedance spectroscopy (EIS) experiments were carried out using a Zahner Zennium workstation and the output signal was acquired with the Thales Z (Zennium release) soft ware. The frequency was ranged from 0.1 Hz to 100,000 Hz with the signal amplitude of 5 mV.

2.3. Preparation of the rGO solution

Graphite oxide was synthesized using graphite powders by the modified Hummer's method [43]. Briefly, 5.0 g graphite powder was dispersed in a 120 mL concentrated H_2SO_4 kept at 0 °C under stirring. Then, 15.0 g of $KMnO_4$ was added gradually to the mixture kept in an ice bath to ensure that the temperature remained around 0 °C. After that, the temperature was raised to 0 °C and the mixture was stirred for 30 min and then diluted gradually with 225 mL deionized water.

The mixture was re-diluted with 700 mL deionized water and treated with 3% hydrogen peroxide. The color of mixture changed to yellow-brown during the dropwise addition of H_2O_2. The mixture was filtered and washed with HCl solution (5%) and then repeatedly washed with water until neutral pH was obtained for filtrate. This solution was centrifuged at 3000 rpm for 10 min and then the filtrate was re-dispersed in water and centrifuged for several times.

Then, the dark brown GO powder was obtained through drying at 50 °C in a vacuum oven for a day. The graphite oxide was then exfoliated by ultra-sonication. Finally, GO powder dispersed in

a known volume of water was subjected to ultra-sonication for 60 min to give a stable suspension of GO and then centrifuged at 3000 rpm for 30 min to remove any aggregates remained in the transparent light brown exfoliated GO suspension. Then, 25mL malt was added into 40 mL above solution and the solution was mixed by ultrasonication for 30 min. The mixture was transferred into a Teflon-lined stainless steel autoclave, and reacted at 90° C for 5 h. During this process, the color of the solution changed from yellow-brown to black. Adsorbed phenolic componds on reduced graphene oxide solution were extracted with ethanol and water by sonication and filtration condition, until no phenolic componds could be detected from the washing solvent with UV-Vis spectrometer. The scheme 1 illustrates the reduction mechanism of GO to rGO by phenolic compounds in malt. Base of this mechanism, the phenolic comopounds oxidized to quinine form at 90°C and release two electrons. These electrons convert the graphene oxide to reduced graphene oxide, suggesting that annealing removed oxygenated groups from the exfoliated graphene oxide sheets.

<Scheme.1>

2.4. Preparation of rGO modified GC electrodes

The end surface of a GC electrode (i.d. = 3.0 mm, Metrohm, Herisau, Switzerland) was polished on a synthetic cloth successively with 0.3, 0.1 and 0.05 µm alumina slurry (Struers, Copenhagen, Denmark) to obtain a mirror finish and then cleaned in water-ethanol solution (1:1) under ultrasonication. A volume of 5µL of the resulting rGO solution was dropped onto a GC electrode and allowed to dry in ambient air for 2 h.

3. Results and Discussion

3.1. Characterization of the composites

We monitored UV-vis absorption spectroscopy exfoliated GO (a) and rGO (b), firstly. As shown in Figure 1.A, the absorption peak at 230 nm showed red-shift to 265 nm after the exfoliated GO is reduced, indicating that the electronic conjugation within the rGO sheets was revived upon reduction of GO [11-14, 19, 20, 43, 44]. The change in color from light brown to black can be seen as the reduction of GO proceeds (Figure 1.A, inset). This color change has previously been suggested as partial restoration of the π network within the carbon structure and has been witnessed through chemical reduction of the exfoliated GO sheets.

The obtained composites are characterized by XRD. As shown in Figure 1.B, the XRD pattern of exfoliated GO (a) exhibits a diffraction peak centered at $2\theta=13.01^{\circ}$, corresponding to the C(002) interlayer spacing of 0.78 nm, which indicates the complete oxidation of graphite to exfoliated GO [45]. After chemical reduction with malt, the diffraction peak of exfoliated GO at $2\theta = 13.01^{\circ}$ disappeared and a very broad peak around 23° (b) was observed in the rGO sample, indicating that most oxygen functional groups had been removed [11, 14, 46, 47]. It should be noted that the diffraction peak in rGO sheets was rather broad and significantly different from that in graphite (Figure 1.B, inset) [45, 48].

Raman spectroscopy is one of the most widely used techniques for the characterization of structural and electronic properties of graphene. In the Raman spectrum of highly ordered graphite a couple of absorption bands, so called G and K bands, are observed at frequencies less than 2000 cm^{-1}. The G band is usually assigned to the E_2g phonon of C sp^2 atoms, the in-phase vibration of the graphite lattice, and it is papered at about 1575 cm^{-1} and represents the relative

degree of graphitization. But, the D band is a weak breathing mode of K-point phonons of A_1g symmetry, caused by the graphite edges and it is appeared at approximately 1355 cm^{-1} and its intensity is related to the degree of edge chirality [49]. Therefore, the ratio of D and G band intensities indicates the degree of the disorder such as defects, ripples and edges. The structural changes from exfoliated GO to rGO sheets occurring during the reduction process are also reflected in their Raman spectra. Figure 1.C shows that the Raman spectrum of exfoliated GO (a) sheets displays a disorder induced D-band around 1350 cm^{-1}, and a G-band around 1590 cm^{-1} due to phonon vibrations in sp^2 carbon materials [50]. After being reduced by malt, the D/G intensity ratio increased from 0.91 to 1.21, suggesting that annealing removed oxygenated groups from the exfoliated GO sheets [51].

< Figure.1>

FTIR spectroscopy was employed to investigate the functional groups of exfoliated GO and rGO. Figure S.1 (Supporting Information) shows the FTIR spectra of those two materials. Figure S.1(A) (Supporting Information) is typical FTIR spectra of deeply oxidized carbon material, as featured for exfoliated GO by a strong absorption band at 1625, 1727 and 3400 cm^{-1} due to C=C, C=O and O-H stretching respectively [11]. However, as shown in Figure S.1(B) (Supporting Information), after the exfoliated GO is chemically reduced, the characteristic absorption bands of oxide groups decreased, indicating that exfoliated GO has been converted to rGO.

The morphologic characterization of the prepared composites was firstly examined by AFM. Figure S.2 (Supporting Information) shows the typical AFM image of exfoliated GO (A) and rGO (B) on the mica, where the cross-sectional view indicates that the average thickness of exfoliated GO nanosheet is about 2.9 nm (Figure S.2.A, Supporting Information). After the final

reduction step, this value decreased to about 0.76 nm (Figure S.2.B, Supporting Information), which could be explained by the removal of the surface oxide groups.

SEM and TEM images of rGO were also given. The obtained SEM image is shown in Figure 2.A. It can be seen that the basic shape of the rGO looks like a piece of a leave structure. Also, Figure 2.B shows a TEM image of rGO sheet. It is evident that the prepared rGO is transparent, wrinkle and flake-like sheet.

< Figure.2>

3.2. Electrochemical properties of the electrodes

EIS has been used to characterize the interface properties of surface-modified electrodes. The typical impedance spectrum (presented in the form of the Nyquist plot) includes a semicircle portion at higher frequencies corresponding to the charge transfer limited process and a linear part at lower frequency range representing the diffusion limited process.

The semicircle diameter in the impedance spectrum equals the charge transfer resistance (R_{ct}). This resistance controls the charge transfer kinetics of the redox probe at the electrode interface. Figure 3 displays the Nyquist plots obtained for a GC (a), rGO /GC (b) and GO/GC (c) electrodes in a solution containing 5.0 mM $Fe(CN)_6^{-3/-4}$ couple (1:1) and 0.1 M KCl, respectively. The Nyquist diameter (R_{ct}) of rGO/GC electrode was much less than these observed for GC and GO/GC electrodes, suggesting that rGO facilitates the rate of charge transfer.

<Figure.3>

3.3 Electrochemical application of rGO

Figure 4.A shows CVs for the oxidation of NADH at these GC (a) and rGO/GC (b) electrodes. After modification with rGO, a remarkable decrease of oxidation peak was achieved. The peak potential of NADH oxidation is shifted from 0.60 V on GC electrode to 0.32 V on rGO/GC

electrode. This synergetic electrocatalytic activity toward NADH could be due to high conductivity, high surface area of rGO and π-π stacking interaction between analyte with this composite. The OH and COH groups on rGO sheet can also form strong hydrogen bonding interaction with OH and NH_2 groups in NADH [52]. Figure 4.B displays the influence of scan rate on the current response for the anodic current of 0.2 mM NADH. The anodic peak current (i_{pa}) increased upon the increase of the square root of scan rate ($\nu^{1/2}$). A good linearity between peak current and $\nu^{1/2}$ was obtained within the range of 10–150 mV/s. The result indicates that the electrochemical kinetics is controlled by the diffusion of NADH.

The Tafel slope can be obtained by following equation that is valid for a totally irreversible diffusion controlled process [53]: $E_p = b/2 \log(\nu) + \text{constant}$ where b indicates the Tafel slope. According to this equation, the evaluated slope of E_p versus $\log(\nu)$ is -0.0536 V decade^{-1}; therefore, b= 0.107 V decade^{-1}. So the amount of transfer coefficient (α) was estimated 0.36 (Figure 4.C).

<Figure.4>

The amperometric responses of biosensor were also investigated by successive addition of NADH to a continuous stirring at the applied potential of 0.32 V versus $Ag|AgCl|KCl_{sat}$ (Figure 5.A). The current responses of the biosensor increased with the concentrations of NADH and reached a steady state within 3 s. It showed that the current responses of GC electrode (a) were relatively small compared with that of the rGO/GC electrode (b). The calibration curve of rGO/GC electrode gave a linear range of the concentration of NADH from 10 µM to 600 µM (insert of Figure 5.A). The linear regression equation was i (µA) = 0.0124 [NADH] (µM) +0.869 with a correlation coefficient of 0.995 (n = 16). From the slope of the resulting calibration curve,

a detection limit of 0.33 μM was estimated at signal-to-noise ratio of 3. The validation parameters for rGO/GC electrode are summarized in Table 1.

<Table.1>

Figure 5.B shows the chronoamperometric measurements of various concentrations of NADH at rGO/GCE by setting the working electrode potential at 0.32 V. Inset of Figure 5.B shows the current responses of different concentrations of NADH. It can be seen from plot that a good liner relationship was realized between the currents and concentrations of NADH. Also, chronoamperometry can be used for the evaluation of the catalytic reaction rate constant (k_{cat}) using the following equation $I_{cat}/I_L = \pi^{1/2}(k_{cat}C_o t)^{1/2}$ [54]. I_{cat} is the catalytic current of the rGO/GC electrode in the presence of NADH, I_L is the limiting current in the absence of NADH, and k_{cat}, C_o, and t are the catalytic rate constant ($M^{-1}.s^{-1}$), bulk concentration (M) and time elapsed (s), respectively. From the slope of the I_{cat}/I_L versus $t^{1/2}$ plot we can simply calculate the value of k_{cat} for a given concentration of substrate. The average value of k_{cat} for a chemical reaction of NADH at rGO/GC electrode was found to be $0.62\times10^5 cm^{-3}\ s^{-1}$ (Figure 5 .B).

For an electroactive material with a diffusion coefficient D the current response under condition of diffusion control is described by Cottrell equation [4] $I= nFACD^{1/2}/ (\pi t)^{1/2}$, where n is the number of electrons; F is the Faraday constant; A is the electrode area; C is the bulk concentration of analyte; D is the diffusion coefficient of analyte in solution; t is the time. In that case, D can be determined from the slope of $I–t^{-1/2}$ curve. The average diffusion coefficient of NADH was calculated to be $1.04\times10^{-7}\ cm^2\ s^{-1}$. The estimated diffusion coefficient is smaller than theoretical value, indicating the efficient electrochemical oxidation of NADH on the surface of electrode.

< Figure.5>

The sensor characteristics compared with other graphene modified electrodes used in the electrochemical determination of NADH are summarized in Table 2. It can be seen that the detection limit of and the peak potential of NADH oxidation in this proposed sensor is better than the Au–RGO/Chit modified GC electrode. These results can be associated with the more efficient electrocatalatic effect of rGO in NADH oxidation. Therefore, malt can be a good reducing agent for the fabrication of cheap and novel rGO that it can be used to make rGO/GC electrode.

< Table 2>

When not in use, the rGO/GC electrode was stored at room temperature in PB solution. No obvious change for CV response was observed after 2 weeks. But after 1 month, its CV decreased by approximately 5.4% (Figure S.3.A, Supporting Information). The proposed sensor was also used for the determination of NADH in urine sample. Briefly, 2.0 mL of the filtered urine solution added to 8.0 mL of PB solution (0.1 M, pH 7.0). Then, the solution was transferred into the voltammetric cell to be analyzed. After that, 10 µL of NADH (0.1 M) injected to this cell and amperometric analysis has done by proposed sensor (Figure S.3.B, Supporting Information). The recovery of the analysis was about 97%, considering the value determined by standard method [55].

4. Conclusion

In this study, we proposed the one-step synthesis of rGO by using malt as an efficient reducing agent. UV-vis, FT-IR, Raman and XRD spectra indicate converting GO to rGO via ec-friendly chemical reduction method. The final reduced graphene oxide composite shows higher

electrochemical activity towards NADH. All these characteristics suggest that rGO composite synthesized by malt is suitable material for fabricating the biosensors.

Acknowledgement

We would like to thank Dr. Behzad Haghighi for all his advice. The authors thank Dr P. Marashi from Maharfan Abzar Co (Tehran, Iran) for the support with the AFM system.

Supporting Information Available:

Supplementary data associated with this article can be found in the online version.

References

[1] Novoselov KS, Geim AK, Morozov SV, Jiang D, Zhang Y, Dubonos SV, Grigorieva IV, Firsov AA. Electric Field Effect in Atomically Thin Carbon Films. Science 2004;306:666-669.

[2] Kim KS, Zhao Y, Jang H, Lee SY, Kim JM, Kim KS, Ahn J-H, Kim P, Choi J-Y, Hong BH. Large-scale pattern growth of graphene films for stretchable transparent electrodes. Nature 2009;457:706-710.

[3] Hamilton CE, Lomeda JR, Sun Z, Tour JM, Barron AR. High-Yield Organic Dispersions of Unfunctionalized Graphene. Nano Letters 2009;9:3460-3462.

[4] Lotya M, King PJ, Khan U, De S, Coleman JN. High-Concentration, Surfactant-Stabilized Graphene Dispersions. ACS Nano 2010;4:3155-3162.

[5] Choucair M, Thordarson P, Stride JA. Gram-scale production of graphene based on solvothermal synthesis and sonication. Nat Nano 2009;4:30-33.

[6] Stankovich S, Dikin DA, Dommett GHB, Kohlhaas KM, Zimney EJ, Stach EA, Piner RD, Nguyen ST, Ruoff RS. Graphene-based composite materials. Nature 2006;442:282-286.

[7] Stankovich S, Dikin DA, Piner RD, Kohlhaas KA, Kleinhammes A, Jia Y, Wu Y, Nguyen ST, Ruoff RS. Synthesis of graphene-based nanosheets via chemical reduction of exfoliated graphite oxide. Carbon 2007;45:1558-1565.

[8] Gao X, Jang J, Nagase S. Hydrazine and Thermal Reduction of Graphene Oxide: Reaction Mechanisms, Product Structures, and Reaction Design. The Journal of Physical Chemistry C 2009;114:832-842.

[9] Huang Y, Liang J, Chen Y. The application of graphene based materials for actuators. Journal of Materials Chemistry 2012;22:3671-3679.

[10] Zhang Y, Nayak TR, Hong H, Cai W. Graphene: a versatile nanoplatform for biomedical applications. Nanoscale 2012;4:3833-3842.

[11] Xie X, Zhao K, Xu X, Zhao W, Liu S, Zhu Z, Li M, Shi Z, Shao Y. Study of Heterogeneous Electron Transfer on the Graphene/Self-Assembled Monolayer Modified Gold Electrode by Electrochemical Approaches. the journal of physical chemistry c 2010;114:14243–14250.

[12] Liu J, Fu S, Yuan B, Li Y, Deng Z. Toward a Universal "Adhesive Nanosheet" for the Assembly of Multiple Nanoparticles Based on a Protein-Induced Reduction/Decoration of Graphene Oxide. Journal of the American Chemical Society 2010;132:7279-7281.

[13] Wang Y, Zhang P, Fang Liu C, Zhan L, Fang Li Y, Huang CZ. Green and easy synthesis of biocompatible graphene for use as an anticoagulant. RSC Advances 2012;2:2322-2328.

[14] Zhang S, Shao Y, Liao H, Engelhard MH, Yin G, Lin Y. Polyelectrolyte-Induced Reduction of Exfoliated Graphite Oxide: A Facile Route to Synthesis of Soluble Graphene Nanosheets. ACS Nano 2011;5:1785-1791.

[15] Pham TA, Kim JS, Kim JS, Jeong YT. One-step reduction of graphene oxide with l-glutathione. Colloids and Surfaces A: Physicochemical and Engineering Aspects 2011;384:543-548.

[16] Thakur S, Karak N. Green reduction of graphene oxide by aqueous phytoextracts. Carbon 2012;50:5331-5339.

[17] Haghighi B, Tabrizi MA. Green-synthesis of reduced graphene oxide nanosheets using rose water and a survey on their characteristics and applications. RSC Advances 2013;3:13365-13371.

[18] Nicolas Segebarth R-MA-S, Eleni Skordi Analysis and Characterisation of Alcoholic Products (ACAP) 2008.

[19] Andersen ML, Outtrup H, Skibsted LH. Potential Antioxidants in Beer Assessed by ESR Spin Trapping. Journal of Agricultural and Food Chemistry 2000;48:3106-3111.

[20] Vinson JA, Mandarano M, Hirst M, Trevithick JR, Bose P. Phenol Antioxidant Quantity and Quality in Foods: Beers and the Effect of Two Types of Beer on an Animal Model of Atherosclerosis. Journal of Agricultural and Food Chemistry 2003;51:5528-5533.

[21] Marova I, Parilova K, Friedl Z, Obruca S, Duronova K. Analysis of Phenolic Compounds in Lager Beers of Different Origin: A Contribution to Potential Determination of the Authenticity of Czech Beer. Chromatographia 2011;73:83-95.

[22] Plazzon A, Forte M, Nardini A. Characterizationof PhenolicsContent andAntioxidant Activity of Different Beer Types. J Agric Food Chem 2010;58:10677-10683.

[23] Tejero I, Gonzalez-Garca Nr, Gonzalez-Lafont, Lluch JEM. Tunneling in Green Tea: Understanding the Antioxidant Activity of Catechol-Containing Compounds. A Variational Transition-State Theory Study. Journal of the American Chemical Society 2007;129:5846-5854.

[24] Rao A, Mahajan K, Bankar A, Srikanth R, Kumar AR, Gosavi S, Zinjarde S. Facile synthesis of size-tunable gold nanoparticles by pomegranate (Punica granatum) leaf extract: Applications in arsenate sensing. Materials Research Bulletin 2013;48:1166-1173.

[25] Das S, Roy P, Mondal S, Bera T, Mukherjee A. One pot synthesis of gold nanoparticles and application in chemotherapy of wild and resistant type visceral leishmaniasis. Colloids and Surfaces B: Biointerfaces 2013;107:27-34.

[26] Inbathamizh L, Ponnu TM, Mary EJ. In vitro evaluation of antioxidant and anticancer potential of Morinda pubescens synthesized silver nanoparticles. Journal of Pharmacy Research 2013;6:32-38.

[27] Zhu H, Du M, Zou M, Xu C, Li N, Fu Y. Facile and green synthesis of well-dispersed Au nanoparticles in PAN nanofibers by tea polyphenols. Journal of Materials Chemistry 2012;22:9301-9307.

[28] Shan C, Yang H, Han D, Zhang Q, Ivaska A, Niu L. Electrochemical determination of NADH and ethanol based on ionic liquid-functionalized graphene. Biosensors and Bioelectronics 2010;25:1504-1508.

[29] Tang L, Wang Y, Li Y, Feng H, Lu J, Li J. Preparation, structure, and electrochemical properties of reduced graphene sheet films. Advanced Functional Materials 2009;19:2782-2789.

[30] Zhou M, Zhai Y, Dong S. Electrochemical Sensing and Biosensing Platform Based on Chemically Reduced Graphene Oxide. Analytical Chemistry 2009;81:5603-5613.

[31] Lin W-J, Liao C-S, Jhang J-H, Tsai Y-C. Graphene modified basal and edge plane pyrolytic graphite electrodes for electrocatalytic oxidation of hydrogen peroxide and β-nicotinamide adenine dinucleotide. Electrochemistry communications 2009;11:2153-2156.

[32] Chang H, Wu X, Wu C, Chen Y, Jiang H, Wang X. Catalytic oxidation and determination of NADH using self-assembly hybrid of gold nanoparticles and graphene. Analyst 2011;136:2735-2740.

[33] Guo K, Qian K, Zhang S, Kong J, Yu C, Liu B. Bio-electrocatalysis of NADH and ethanol based on graphene sheets modified electrodes. Talanta 2011;85:1174-1179.

[34] Li Y, Yang X, Yang F, Wang Y, Zheng P, Liu X. Effective immobilization of Ru(bpy)32+ by functional composite phosphomolybdic acid anion on an electrode surface for solid-state electrochemiluminescene to sensitive determination of NADH. Electrochimica Acta 2012;66:188-192.

[35] Dilgin DG, Gligor D, Gökçel Hİ, Dursun Z, Dilgin Y. Photoelectrocatalytic oxidation of NADH in a flow injection analysis system using a poly-hematoxylin modified glassy carbon electrode. Biosensors and Bioelectronics 2010;26:411-417.

[36] Rex A, Fink F. Applications of laser-induced fluorescence spectroscopy for the determination of NADH in experimental neuroscience. Laser Physics Letters 2006;3:452-459.

[37] Brugidou C, Rocher A, Giraud E, Lelong B, Marin B, Raimbault M. A new high performance liquid chromatographic technique for separation and determination of adenylic and nicotinamide nucleotides in Lactobacillus plantarum. Biotechnol Tech 1991;5:475-478.

[38] Gasnier A, Laura Pedano M, Rubianes MD, Rivas GA. Graphene paste electrode: Electrochemical behavior and analytical applications for the quantification of NADH. Sensors and Actuators B: Chemical 2013;176:921-926.

[39] Guo K, Qian K, Zhang S, Kong J, Yu C, Liu B. Bio-electrocatalysis of NADH and ethanol based on graphene sheets modified electrodes. Talanta 2011;85:1174-1179.

[40] Li L, Lu H, Deng L. A sensitive NADH and ethanol biosensor based on graphene–Au nanorods nanocomposites. Talanta 2013;113:1-6.

[41] Li Z, Huang Y, Chen L, Qin X, Huang Z, Zhou Y, Meng Y, Li J, Huang S, Liu Y, Wang W, Xie Q, Yao S. Amperometric biosensor for NADH and ethanol based on electroreduced graphene oxide–polythionine nanocomposite film. Sensors and Actuators B: Chemical 2013;181:280-287.

[42] Tabrizi MA, Zand Z. A Facile One-Step Method for the Synthesis of Reduced Graphene Oxide Nanocomposites by NADH as Reducing Agent and Its Application in NADH Sensing. Electroanalysis 2014;26:171-177.

[43] Hummers WS, Offeman RE. Preparation of Graphitic Oxide. Journal of the American Chemical Society 1958;80:1339-1339.

[44] Zhou Y, Bao Q, Tang LAL, Zhong Y, Loh KP. Hydrothermal Dehydration for the "Green" Reduction of Exfoliated Graphene Oxide to Graphene and Demonstration of Tunable Optical Limiting Properties. Chemistry of Materials 2009;21:2950-2956.

[45] Guo H-L, Wang X-F, Qian Q-Y, Wang F-B, Xia X-H. A Green Approach to the Synthesis of Graphene Nanosheets. ACS Nano 2009;3:2653-2659.

[46] Hassan HMA, Abdelsayed V, Khder AERS, AbouZeid KM, Terner J, El-Shall MS, Al-Resayes SI, El-Azhary AA. Microwave synthesis of graphene sheets supporting metal nanocrystals in aqueous and organic media. Journal of Materials Chemistry 2009;19:3832-3837.

[47] McAllister MJ, Li J-L, Adamson DH, Schniepp HC, Abdala AA, Liu J, Herrera-Alonso M, Milius DL, Car R, Prud'homme RK, Aksay IA. Single Sheet Functionalized Graphene by Oxidation and Thermal Expansion of Graphite. Chemistry of Materials 2007;19:4396-4404.

[48] Yang H, Shan C, Li F, Han D, Zhang Q, Niu L. Covalent functionalization of polydisperse chemically-converted graphene sheets with amine-terminated ionic liquid. Chemical Communications 2009;0:3880-3882.

[49] Tuinstra F, Koenig JL. Raman Spectrum of Graphite. The Journal of Chemical Physics 1970;53:1126-1130.

[50] Kudin KN, Ozbas B, Schniepp HC, Prud'homme RK, Aksay IA, Car R. Raman Spectra of Graphite Oxide and Functionalized Graphene Sheets. Nano Letters 2007;8:36-41.

[51] Ferrari A, Robertson J. Interpretation of Raman spectra of disordered and amorphous carbon. Physical Review B 2000;61:14095-14107.

[52] Tabrizi MA, Zand Z. A Facile One-Step Method for the Synthesis of Reduced Graphene Oxide Nanocomposites by NADH as Reducing Agent and Its Application in NADH Sensing. Electroanalysis 2013;26:171-177.

[53] A.J. Bard LRF, Electrochemical Methods, Fundamentals and Applications, Wiley, New York, 1980.

[54] Z. Galus FoEA, Ellis Horwood, Press NY, 1976, p. 313 (Chapter 10).

[55] T. Ohno MS, T. Horiuchi, Y. Shirahase, K. Kishi, Y., Watazu USPUA, Oct. 5, 1993.

[56] Keeley GP, O'Neill A, Holzinger M, Cosnier S, Coleman JN, Duesberg GS. DMF-exfoliated graphene for electrochemical NADH detection. Physical Chemistry Chemical Physics 2011;13:7747-7750.

Figure captions

Scheme .1. The reduction mechanism of GO.

Figure 1. (A) UV-vis absorption spectra obtained for exfoliated GO (a) and rGO (b) solutions, respectively. Inset: Photograph showing the change in color of exfoliated GO solution (0.07 mg mL^{-1}) before (a) and after (b) reduction with malt. (B) Typical XRD patterns obtained for exfoliated GO (a) and rGO (b), respectively. Inset: XRD pattern for pristine graphite(c). (C) Raman spectra obtained for exfoliated GO (a) and rGO (b) respectively. (The Raman system specifications are as follows: Laser power: 30 mW, laser wavelength: second harmonic @532 nm of a Nd:YLF laser, acquisition time : 32 scans which take something around 3 minutes.)

Figure 2. The SEM image (A) and TEM image (B) of rGO, respectively.

Figure 3. The Nyquist plots obtained for a GC (a) and rGO/GC (b) electrodes in a solution containing 5.0 mM $Fe(CN)_6^{-3/-4}$ couple (1:1) and 0.1 M KCl. Inset: The Nyquist plot obtained for a GO/GC electrode (c) at the same operation conditions stated before.

Figure 4. (A) Cyclic voltammograms of rGO/GC (a) and GC (b) electrodes in 0.1 M PB solution (pH=7.0) containing 0.2 mM NADH, at a scan rate of 0.05 Vs^{-1}, (B) Cyclic voltammograms of

0.2 mM NADH at various square root of scan rate ($\nu^{1/2}$), inset (B) shows the linear dependence of anodic peak currents versus $\nu^{1/2}$ in the range from 10 to 150 Vs^{-1}. (C) Plot of E_p versus log(ν) obtained from cyclic voltammetric experiments for rGO/GC electrode in various scan rate.

Figure 5. (A) Amperometric responses of GC electrode (a) and rGO/GC electrode (b) in 0.1 M PB solution (pH=7.0) to successive additions of NADH; the inset is the calibration curve of rGO/GC electrode, (B) Chronoamperograms obtained at rGO/GC electrode in the absence (dash line) and presence of NADH from 10-100.µM. (C) Plot of I_{cat}/I_L versus $t^{1/2}$ obtained from chronoamperometric experiments for at rGO/GC electrode in PB solution (pH =7.0) containing NADH concentrations of 10, 25, 50, 65, 75 and 100 µM. The operating potential: 0.32 V versus $Ag|AgCl|KCl_{sat}$.

Table.1. The validation parameters for rGO/GC electrode.

LOD	LOQ	Precision[a] (μM)	Accuracy	RSD %	BIAS %	Slope (μA μM^{-1})	Intercept (μA)	SE of slope	SE of intercept
0.53	1.83	0.33±0.02	99.67	0.77	0.326	0.0124	0.869	0.0023	0.0040

a: calculated with 95% confidence limits

LOD: Limit of detection, LOQ: limit of quantitation, RSD: Relative standard deviation,

SE: Standard error,

Table2. Comparison of the performance of the rGO/GC electrode for the electrochemical detection of NADH with that of other rGO modified electrodes.

Working electrode	Applied potential (V) vs. Ag|AgCl	Linear range (μM)	Detection limit (μM)	References
Chemically reduced graphene oxide/GC electrode	+0.45	40–800	10	[30]
Graphene/edge plane pyrolytic graphite electrode	+0.564	-	-	[31]
Ionic liquid functionalized graphene/GC electrode	+0.45	250-2000	5	[28]
Au–RGO/Chit modified GC electrode	+0.35	1.5 to 320	1.2	[32]
GNS/GC electrode	+0.4	0-600	1.4	[56]
rGO/GC electrode	+0.32	10-600	0.33	This work

Figures

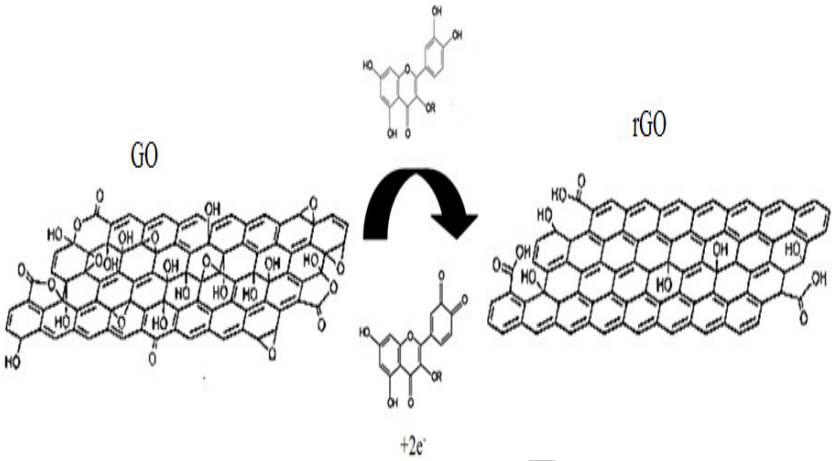

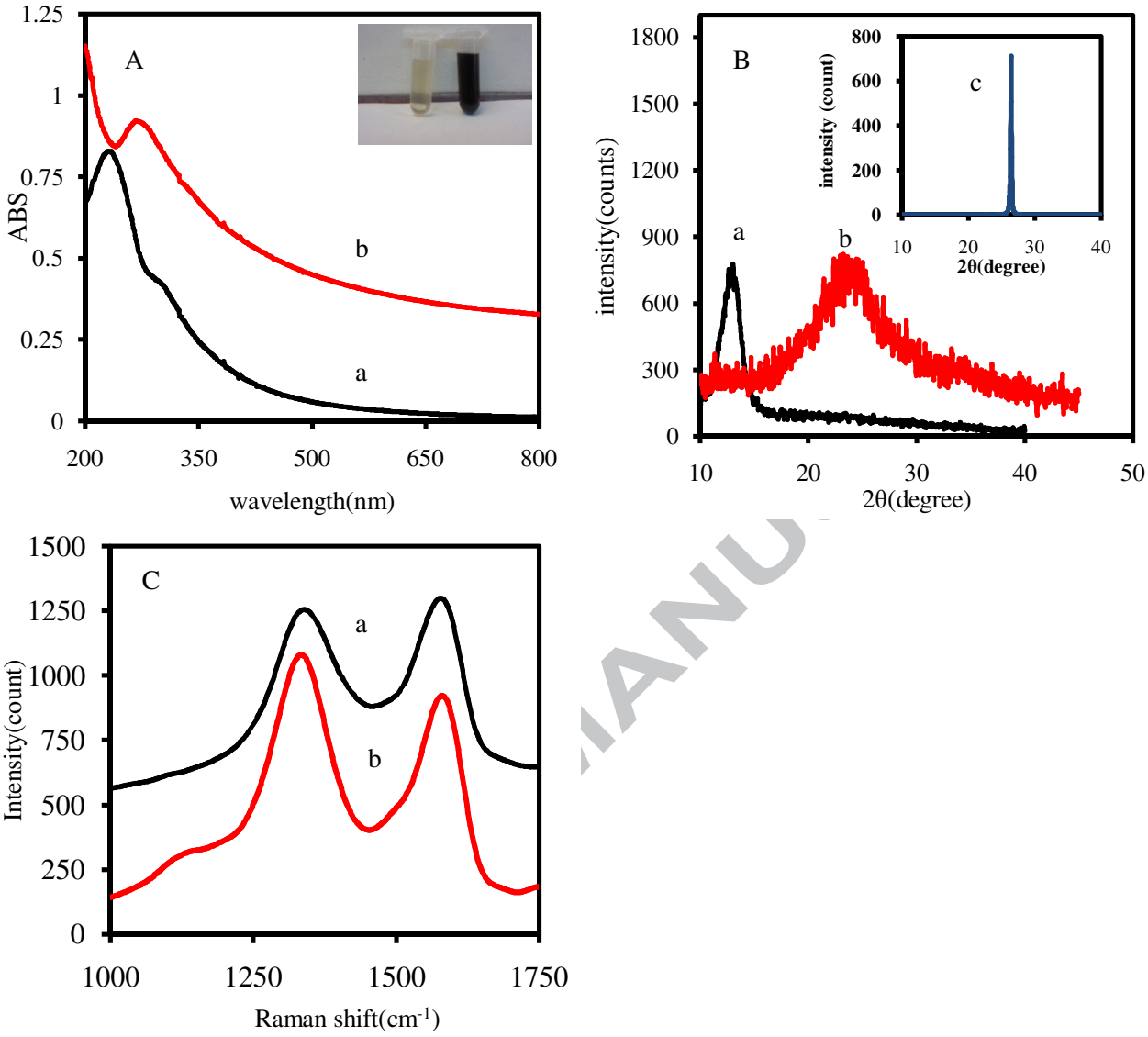

Figure 1.

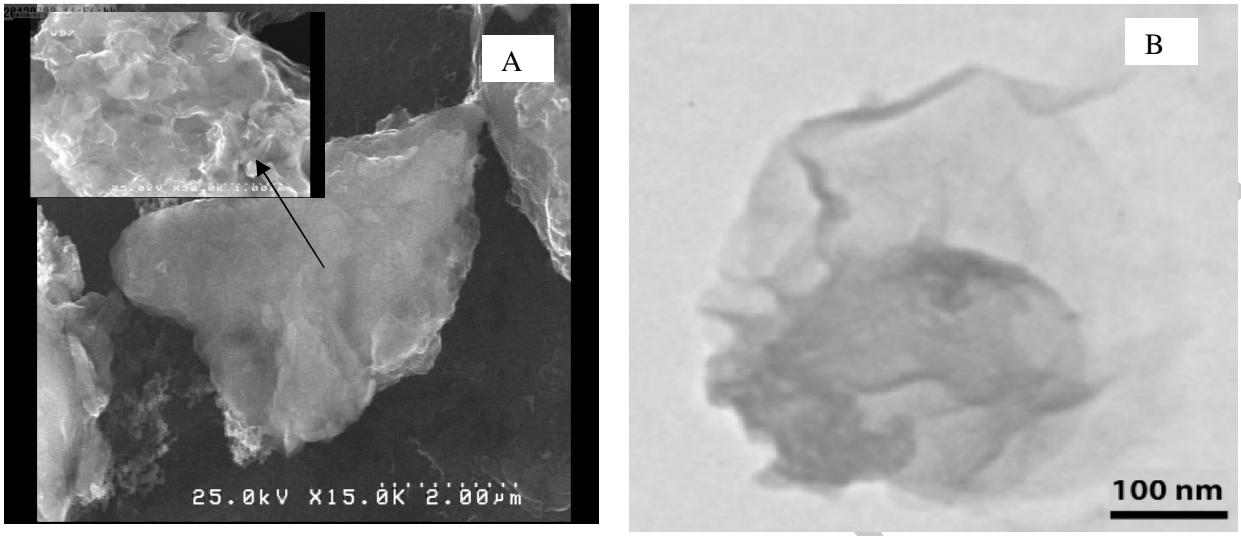

Figure 2.

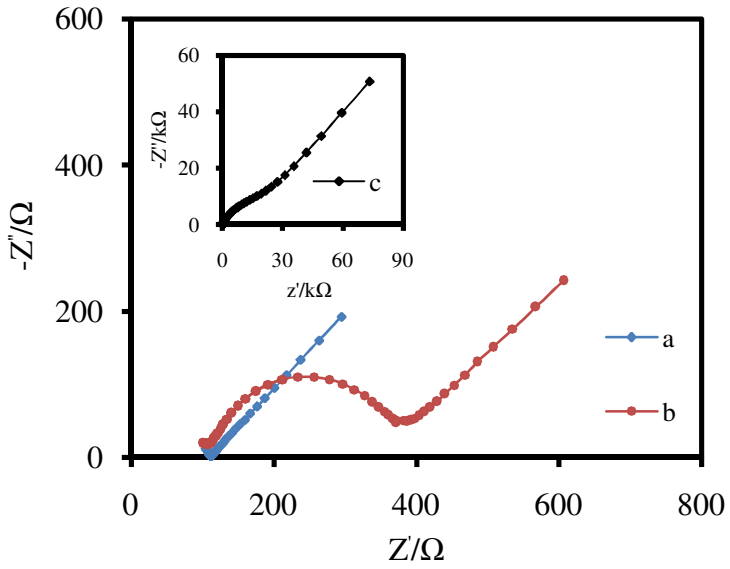

Figure 3.

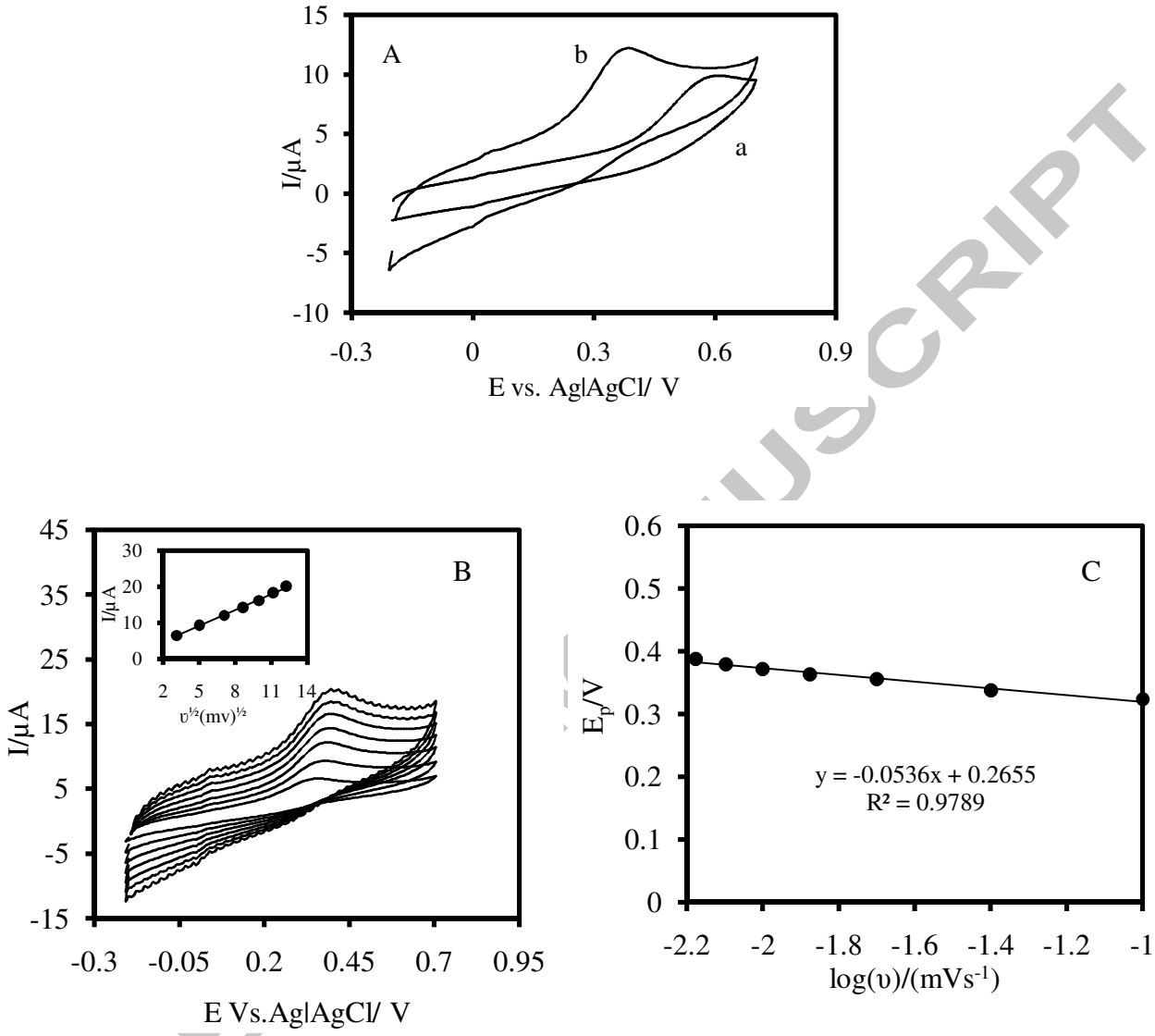

Figure 4.

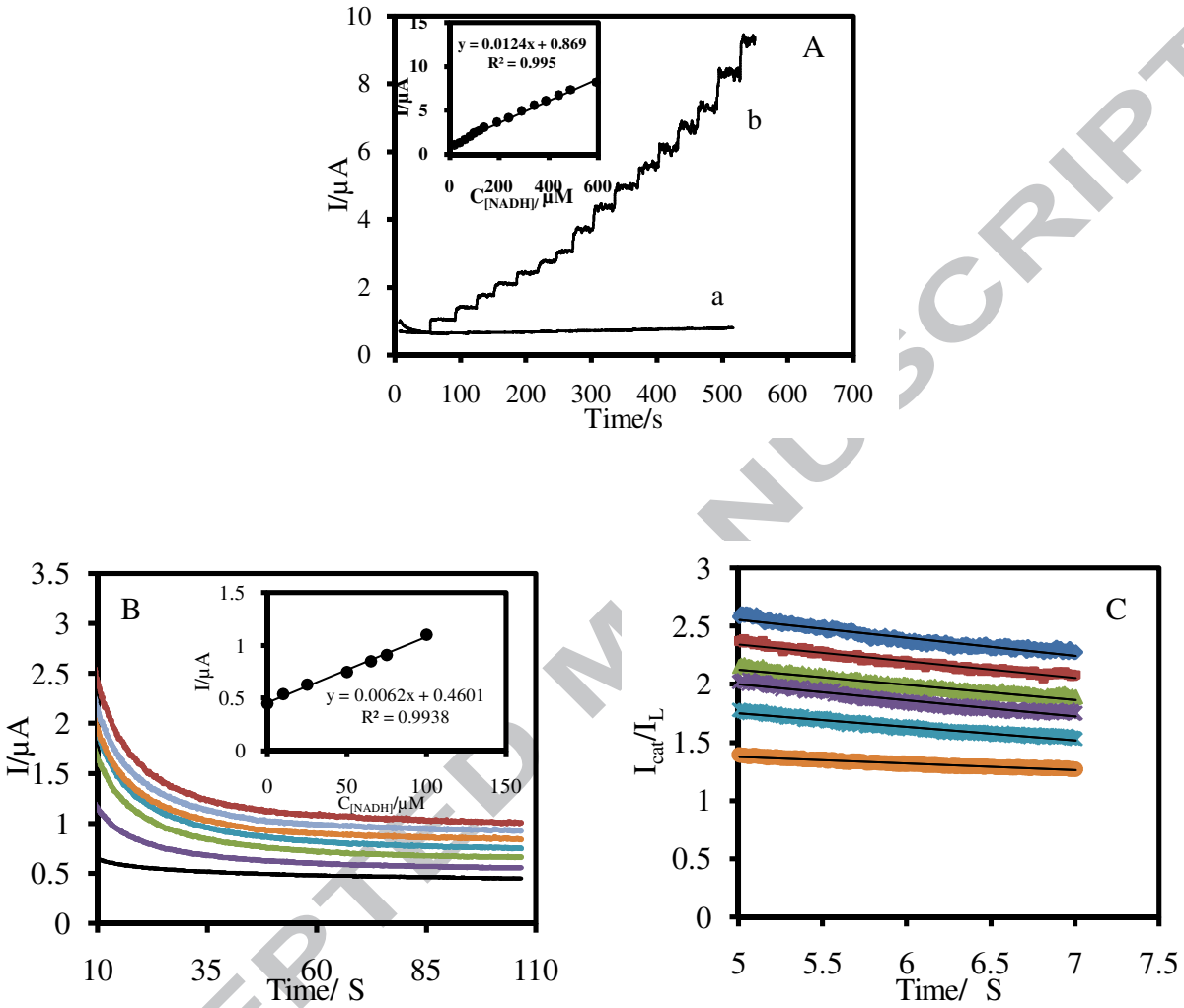

Figure 5.